Naval Research Laboratory

Washington, DC 20375-5320

NRL/MR/5650--06-8996

Beam Divergence from an SMF-28 Optical Fiber

ANDREW M. KOWALEVICZ, JR.
FRANK BUCHOLTZ

Photonics Technology Branch
Optical Sciences Division

October 6, 2006

REPORT DOCUMENTATION PAGE

Form Approved
OMB No. 0704-0188

1. REPORT DATE *(DD-MM-YYYY)*	**2. REPORT TYPE**	**3. DATES COVERED** *(From - To)*
06-10-2006	Memorandum Report	1 July 2005 - 24 August 2006

4. TITLE AND SUBTITLE

Beam Divergence from an SMF-28 Optical Fiber

5a. CONTRACT NUMBER

5b. GRANT NUMBER

5c. PROGRAM ELEMENT NUMBER

6. AUTHOR(S)

Andrew M. Kowalevicz, Jr., and Frank Bucholtz

5d. PROJECT NUMBER

5e. TASK NUMBER

5f. WORK UNIT NUMBER

7. PERFORMING ORGANIZATION NAME(S) AND ADDRESS(ES)

Naval Research Laboratory
4555 Overlook Avenue, SW
Washington, DC 20375-5320

SFA, Inc.
2200 Defense Highway
Crofton, MD 21114

8. PERFORMING ORGANIZATION REPORT NUMBER

NRL/MR/5650--06-8996

9. SPONSORING / MONITORING AGENCY NAME(S) AND ADDRESS(ES)

Office of Naval Research
One Liberty Center
875 North Randolph Street
Arlington, VA 22203-1995

10. SPONSOR / MONITOR'S ACRONYM(S)

ONR

11. SPONSOR / MONITOR'S REPORT NUMBER(S)

12. DISTRIBUTION / AVAILABILITY STATEMENT

Approved for public release; distribution is unlimited.

13. SUPPLEMENTARY NOTES

14. ABSTRACT

We present a calculation and experimental results using three different approaches for the spatial divergence of an optical beam exiting a standard, single-mode telecommunications-grade optical fiber (SMF-28) operating near 1550 nm wavelength. The analysis shows some pitfalls for a common imaging technique for determining beam width and shows good agreement with theory when the beam width measurement is performed using either a knife-edge or pinhole approaches. These results are important for maximizing coupling efficiency between single-mode fibers and photodetectors.

15. SUBJECT TERMS

Optical fiber
Numerical aperture
Beam divergence

16. SECURITY CLASSIFICATION OF:			**17. LIMITATION OF ABSTRACT**	**18. NUMBER OF PAGES**	**19a. NAME OF RESPONSIBLE PERSON**
					Andrew M. Kowalevicz, Jr.
a. REPORT	**b. ABSTRACT**	**c. THIS PAGE**	UL	17	**19b. TELEPHONE NUMBER** *(include area code)*
Unclassified	Unclassified	Unclassified			(202) 767-9365

Standard Form 298 (Rev. 8-98)
Prescribed by ANSI Std. Z39.18

CONTENTS

Executive Summary

An accurate description and model for beam divergence from a fiber is often important in photonics applications. In this paper we characterize the beam divergence from SMF-28 fiber at 1550 nm by three methods: (1) BeamAlyzer, (2) Knife edge scan, and (3) Pinhole power measurements. We compare the experimental data to the Gaussian beam model with the initial beam diameter ($2w_0$) set to the mode-field diameter of the fiber of 10.5 μm. We find that the BeamAlyzer data is unreliable and does not fit the theoretical description. On the other hand, the knife edge scan and the pinhole power measurements show that the Gaussian beam model can be used to accurately and precisely describe the beam divergence to a very high degree. We also see that the manufacturer's specified numerical aperture (NA) is measured in the far field, and differs from the calculated NA based on the core and cladding indices of refraction.

Manuscript approved August 29, 2006.

Introduction

Characteristics such as low-loss, high-bandwidth, and environmental stability make photonic links (networks where information is transmitted through optical fiber) increasingly attractive. Regardless of the means by which information is encoded onto the light, in most cases, said information needs to be converted back into the electrical domain to be useful. The optical-to-electrical conversion is achieved by propagating the light from the end of the fiber, through some distance of free space (where it undergoes diffraction), and onto a photodetector (PD).

Knowledge of the beam size and intensity profile at a given distance is vital to optimizing link design and performance. For single fiber-detector systems, knowledge of the beam specifications allows a more uniform intensity profile to be formed on the PD, which can eliminate the "hot-spot" in high power applications. When a single element is used to detect light from multiple fibers, or bundles, information about the beam ensures that an appropriately sized PD is chosen for sufficient collection efficiency.

Despite the fact that the light inside a step-index fiber actually has a Bessel intensity profile, a convenient approximation has been established to simplify the calculations of the beam parameters as it leaves the fiber. It is generally acceptable to treat the output light as a Gaussian beam, with the initial beam diameter, $2w_0$, set to the mode-field diameter of the fiber (MFD), which is often specified by the manufacturer.

In this paper, we review both the approximation and the exact solution for light inside an SMF-28 fiber. We then use the Gaussian beam approximation to predict beam divergence and integrated power incident on a photodetector of a given size. Results are compared to knife-edge measured beam sizes and observed power transmitted through a small circular pinhole.

Background

Guided Modes in Fibers

Figure 1 shows a schematic representation of the fiber used in the study. It is a step index fiber with an effective group index of refraction of 1.4677 at 1310 nm and 1.4682 at 1550 nm. The core radius, a, is 4.1 μm with a cladding radius, b, of 62.5 μm. The wave is guided because $n_1 > n_2$ with a core/cladding index difference of 0.36%[1].

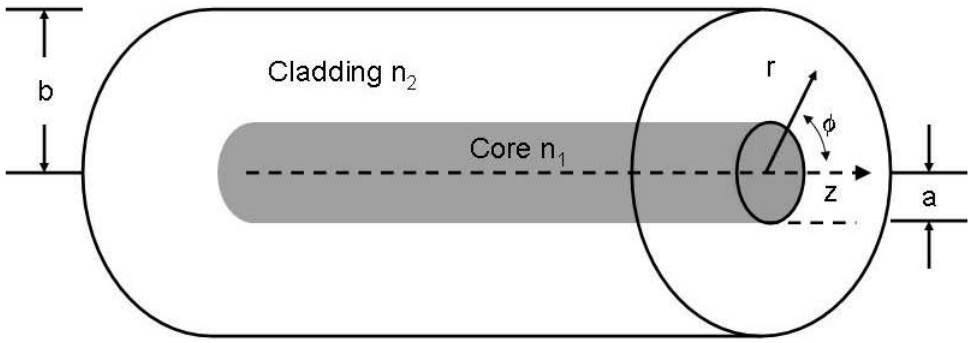

Figure 1. Schematic representation of SMF-28 optical fiber with core radius of a, and cladding radius b. Optical axis of fiber is aligned along the z direction.

The representation of the guided wave can be determined by following a well known analysis[2]. Electromagnetic waves within the fiber satisfy the Helmholtz equation, $\nabla^2 U + n^2 k_0^2 U = 0$. Here $k_0 = 2\pi/\lambda$, with n being n_1 or n_2 depending on whether the equation is applied in the core (r < a) or cladding (r > a) region, respectively. *U* represents the complex amplitude of the electric or magnetic fields in cylindrical coordinates, i.e. *U = U(r, ϕ, z).* Since we are interested in traveling wave solutions along z with a propagation constant, β, and functions in ϕ that are 2π periodic, we can choose *U* such that

$$U(r,\phi,z) = u(r)e^{-il\phi}e^{-i\beta z}, \quad l = 0,\pm1,\pm2,\pm3\ldots \qquad [1]$$

By substituting Eqn. [1] into the Helmholtz equation, we are left with an ordinary differential equation for *u(r),*

$$\frac{d^2u}{dr^2} + \frac{1}{r}\frac{du}{dr} + \left(n^2k_0^2 - \beta^2 - \frac{l^2}{r^2}\right)u = 0\,. \qquad [2]$$

The bound solutions, where the wave is guided, occur when the propagation constant, β, is smaller (larger) than the wavenumber, nk_0, in the core (cladding). For convenience, we may then define,

$$\kappa^2 = n_1^2k_0^2 - \beta^2 \qquad [3a]$$

And

$$\gamma^2 = \beta^2 - n_1^2k_0^2, \qquad [3b]$$

so that κ and γ are real in the core and cladding, respectively. Eqn. [2] can then be written separately for the core and cladding regions. The well known solutions for *u(r)* are then obtained,

$u(r) \propto J_l(\kappa r)$, for r < a (core) [4a]

$u(r) \propto K_l(\gamma r)$, for r > a (cladding). [4b]

$J_l(x)$ is the Bessel function of the first kind, of order l, which oscillates with decreasing amplitude as x increases. $K_l(x)$ is the modified Bessel function of the second kind, of order l, which is a monotonically decreasing function for increasing x.

The boundary conditions dictate that the two solutions for the scalar function $u(r)$, must be continuous with continuous derivatives at the core-cladding interface. Using this fact together with some Bessel function identities, we obtain the characteristic equation for weakly guiding fiber (i.e. where $\Delta n << 1$)

$$\frac{(\kappa a) J_{l\pm1}(\kappa a)}{J_l(\kappa a)} = \pm \gamma a \frac{K_{l\pm1}(\gamma a)}{K_l(\gamma a)}. \quad [5]$$

This equation can be solved graphically by realizing that

$$(\kappa a)^2 + (\gamma a)^2 = (n_1^2 - n_2^2) k_0^2 a^2 = \left(2\pi \frac{a}{\lambda} \mathrm{NA}\right)^2 = \mathrm{V}^2, \quad [6]$$

Where the numerical aperture, $\mathrm{NA} = \sqrt{n_1^2 - n_2^2}$. V is a parameter called the "V-number," which governs number of propagating modes in the fiber.

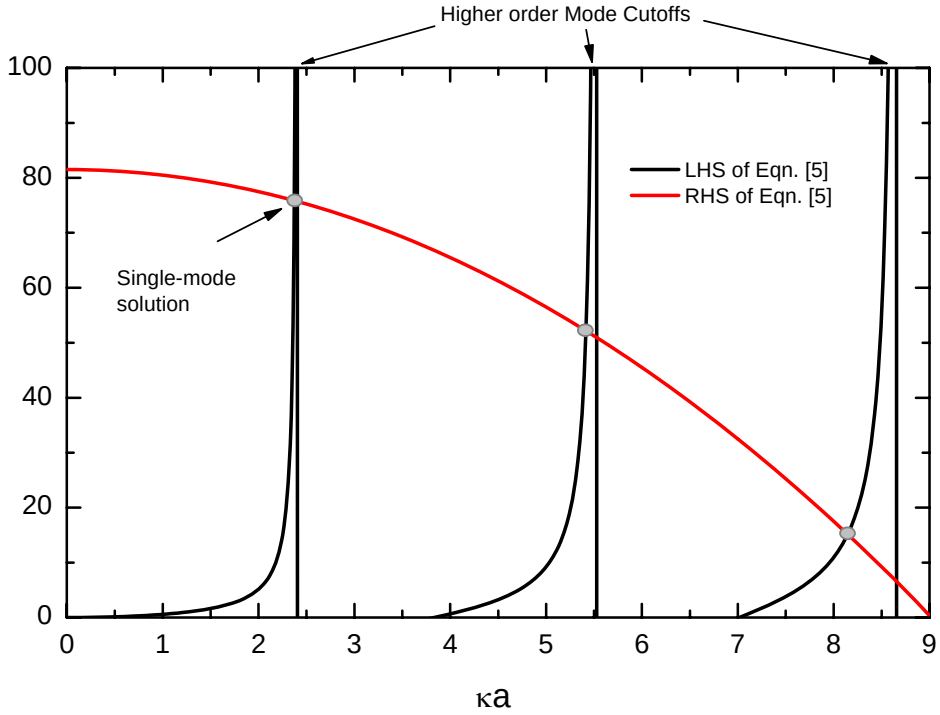

Figure 2. Graphical solution to the characteristic equation, Eqn. [5]. Each point of intersection represents a mode solution. The vertical lines represent V-number cutoffs for higher order modes.

Figure 2 shows a graphical construction for solving the characteristic equation, Eqn. [5]. For the purpose of illustration, we have chosen V = 9 and l = 0. With these parameters, the LHS of [5] has multiple branches, which intersect the abscissa at the roots of $J_1(\kappa a)$. Solutions are found by the intersection of the RHS with the different branches. Each intersection corresponds to one mode. The vertical asymptotes represent the cutoff V-number for each of the higher order modes. For the case of SMF-28, the fiber is designed such that V < 2.405 over its operating wavelengths, so that there is only one point of intersection, making it a "single-mode" fiber.

Beam Divergence

While the electromagnetic wave is propagating inside of the fiber, the guiding properties of the dielectric cancel diffraction effects. Once the beam leaves the fiber, however, the confinement is no longer maintained, and the beam begins to spread. While the diffraction of the Bessel beam exiting the fiber could be evaluated analytically, this calculation is rarely necessary because of its similarity to a fundamental Gaussian beam.

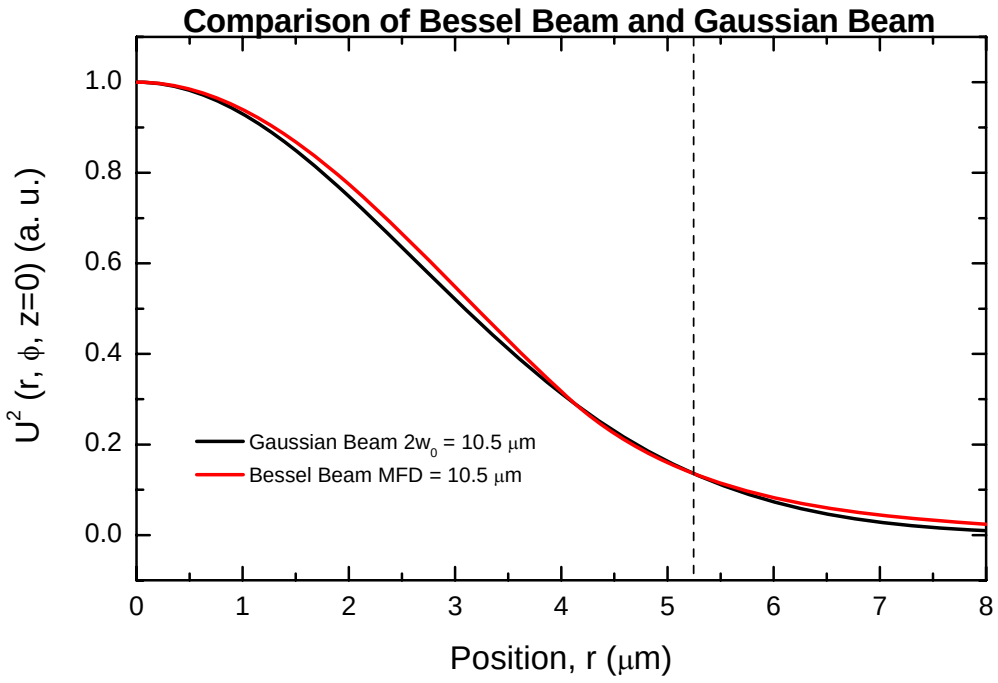

Figure 3. Mode profile of the Bessel beam at the output facet of the SMF-28 fiber with the $1/e^2$ intensity point matched to the mode-field diameter specified by the manufacturer. A Gaussian beam is also plotted for comparison. The beams were set to unity amplitude at r = 0, and to $1/e^2$ intensity at r = MFD (vertical dashed line). The total integrated power of the two profiles in the figure is not equal.

Figure 3 shows the Bessel beam intensity profile with a mode-field diameter of 10.5 μm, compared with the Gaussian approximation for an SMF-28 fiber. The beams were set to unity at r = 0 and to equal values at the $1/e^2$ intensity position, the point where the initial

beam radius, w_0, is specified for a Gaussian beam. It is important to be aware that the manufacturer typically specifies an empirical NA on the data sheets. For the case of interest, the manufacturer specified an NA of 0.14 by measuring the far-field 1% power level. This value differed from the calculated NA of 0.12 given by Eqn. [6]. The latter was needed to get the proper normalization in the near-field and gives a corresponding V-number of 1.76. While it should be noted that the total integrated power of the beams is not equivalent (the Bessel beam in the figure has 10% more total power when integrated over all space), the intensity profiles in the region where most of the power is contained is excellent.

Assuming that the approximation is valid, the beam divergence from the SMF-28 optical fiber can be treated as a Gaussian beam with an initial beam diameter (full $1/e^2$ width), $2w_0$, set equal to the Mode-field diameter (MFD) of the fiber. In this case, the beam radius at a position z, as shown in Figure 4, can be found from[3]

$$w(z) = w_0 \sqrt{1 + \left(\frac{z}{z_R(w_0)} \right)^2}, \qquad [7]$$

where

$$z_R(w_0) = \frac{\pi}{\lambda} w_0^2. \qquad [8]$$

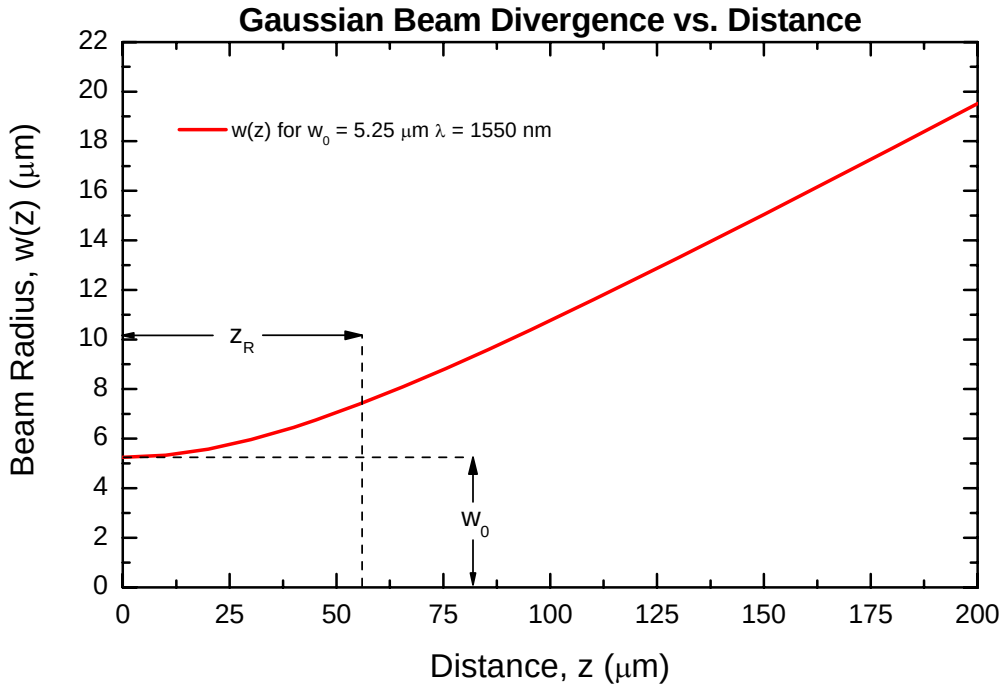

Figure 4. Graphical representation of Eqn. [7] showing the initial beam radius, w_0 = 5.25 μm and the Rayleigh range, z_R, for light with λ = 1550 nm.

Experiment

Beam Profile Measurement

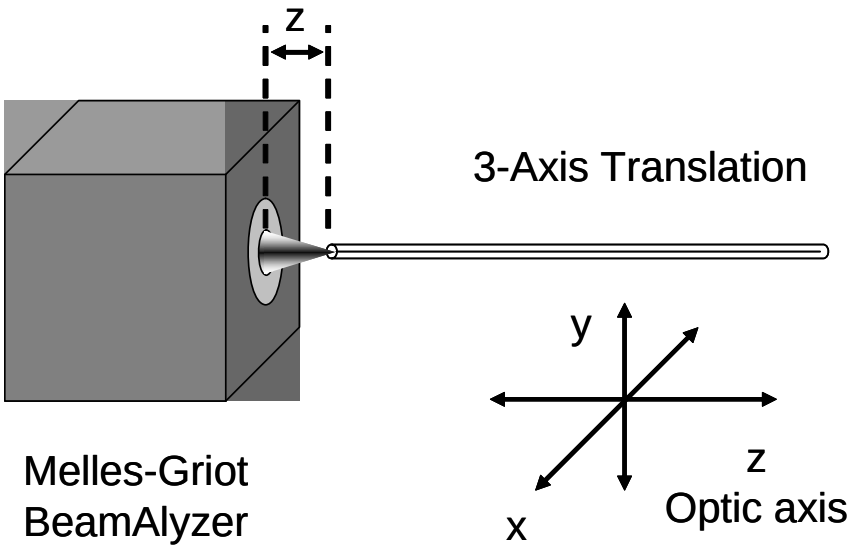

Figure 5. Schematic representation of the beam profile measurement setup. The fiber was positioned by a 3-axis translation stage and aligned with the input aperture of the Melles-Griot Super BeamAlyzer.

In order to compare the theoretical predictions with observed results, we first set up an experiment to measure the beam divergence. We used a JDS Uniphase laser operating at 1.55 μm, which was fusion spliced to SMF-28 fiber. The SMF-28 fiber was wound around a mandrel to eliminate any cladding modes that might have been generated from the imperfect mode match between the polarization maintaining fiber connected to the laser output and the fiber under test.

The end of the SMF-28 fiber was then stripped, cleaned and cleaved to create a good output facet. A Melles-Griot Super BeamAlyzer, with the capability to characterize a beam spot from 3 μm to 3 mm in size, was then used to measure the beam. The beam parameters were evaluated at regular intervals from the scanning slit of the device by translating the fiber on a 3-axis stage parallel to the optic axis, as depicted in Figure 5. Any small deviations in the final beam position were adjusted before each measurement to ensure the beam intersected the profiler at the same point each time. Electronic versions of the intensity profiles were saved for later analysis.

Using the saved intensity profiles, Gaussian intensity envelopes were fit to the data, and beam spot sizes, w, were extracted as shown in Figure 6. For comparison, the actual position where the recorded intensity envelopes crossed the $1/e^2$ level were also found and used to determine the beam size at a given distance.

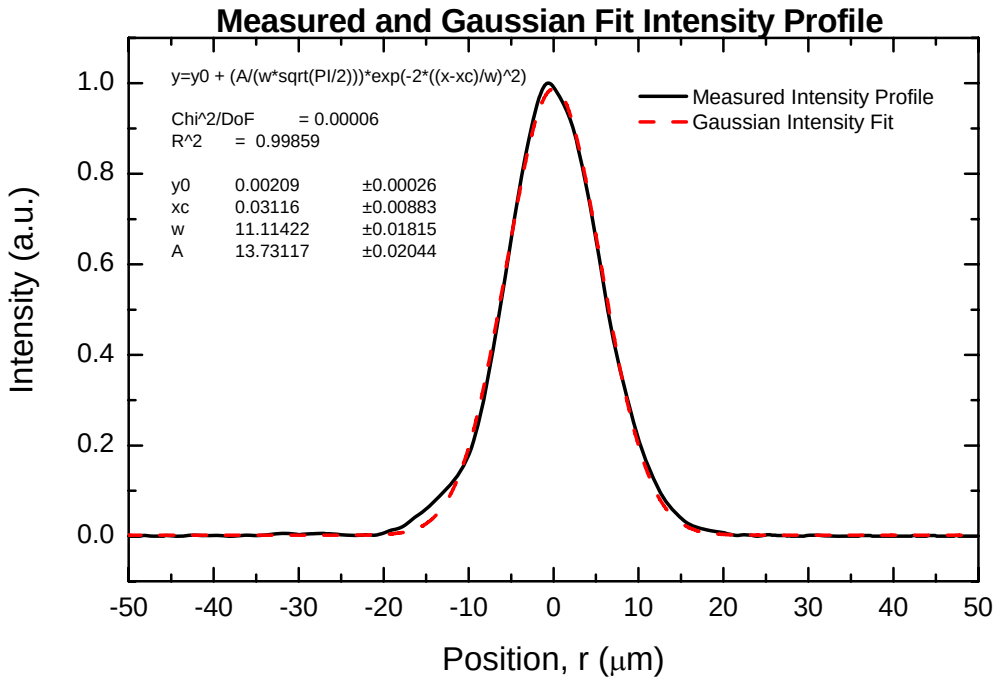

Figure 6. A representative measurement of the intensity profile exiting the SMF-28 fiber as recorded by the BeamAlyzer (Black Solid Line). For comparison and analysis, a Gaussian beam intensity profile was fit to the measured data (Red Dashed Line) and the beam parameters were extracted. The above measurement was performed at the output facet of the fiber (z = 0).

Figure 7 shows a family of curves giving the results of the measurements. In addition to the two sets of data points described above, labeled "Gaussian Fit Width," and "Measured Width," respectively, the plot has three additional curves. During the measurements, the BeamAlyzer continuously makes a determination of the $1/e^2$ beam width that updates on the display in real-time. These numbers were recorded by hand after the screen updates came to steady-state and are labeled "Screen Displayed Width" on the plot. The "Saved Width" shows the values that were saved to the data file by the BeamAlyzer when the intensity profiles were captured. Lastly, the theoretically predicted beam width, based on manufacturer specifications, is also shown on the graph for a Gaussian beam with an initial spot size, $2w_0 = 10.5$ μm.

By examining the graph it becomes clear that there is very good agreement between the "Saved Width", the "Measured Width" and the "Gaussian Fit Width." The fact that these values do not agree with the "Screen Displayed Width" indicates that there is probably a problem in the algorithm that displays the data in real time. A more serious concern is that none of the measurement agrees with what is theoretically predicted.

Even though the Gaussian fits to the recorded intensity envelopes have excellent agreement (Figure 6), the BeamAlyzer measurement of the beam divergence does not correspond to that of a Gaussian beam. The measured spot sizes are not nearly the same

as the predicted values. In addition, they are not simply off by a constant value or multiplicative factor. The Gaussian beam is expected to diverge at a constant rate in the far-field. The divergence shown by any of the curves, antithetically, is sub-linear.

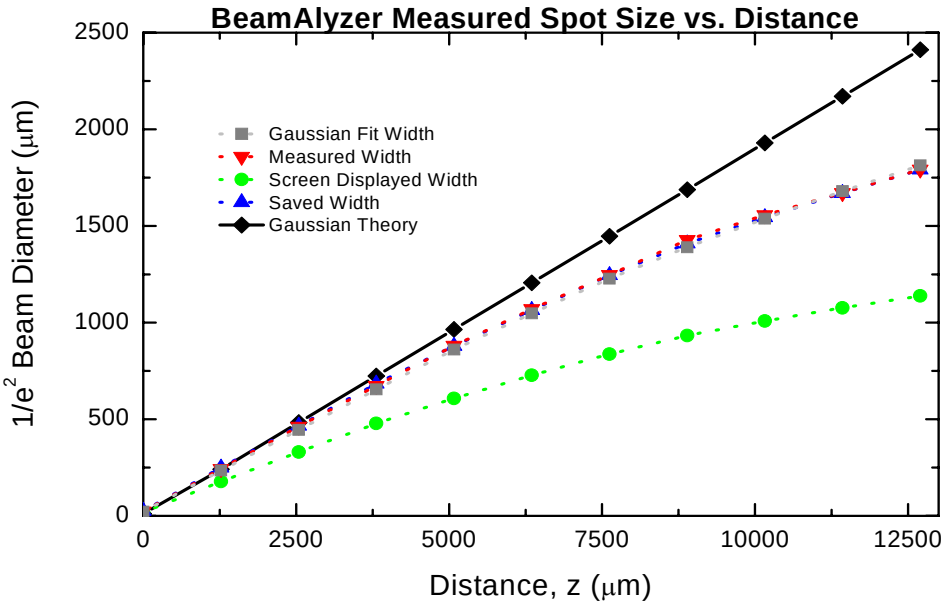

Figure 7. Measurements of the beam divergence from SMF-28 fiber. The plot shows comparison between values measured by the BeamAlyzer, compared with a Gaussian beam divergence for an initial spot size, $2w_0$ = 10.5 μm.

Knife-edge Measurement

Because the automated measurement of the beam divergence led to unexpected results, we set up a second experiment to independently measure beam size. Figure 8 shows a schematic of the setup. The fiber was mounted on a translation stage which was used to position it along the optic axis. By translating a straight edged razor blade into the propagating beam and monitoring the power, the beam size at the position of the blade could be determined.

Assuming a Gaussian shaped intensity pattern, the integrated power at the intensity points at 13.5% ($1/e^2$) of the peak were calculated to be 2.3% and 97.7%. Since these values were close to the null (0%) and maximum power (100%) points, it was decided that more reliable data could be obtained if the full-width at half the maximum (FWHM) intensity was measured. The FWHM corresponds to the 12.0% and 88.0% power points. From this width, the $1/e^2$ points can be inferred from the relation

$$w = \sqrt{\frac{2}{\ln 2}}\sigma \qquad [9]$$

where w is the $1/e^2$ beam radius, and σ is the half width at half maximum power point.

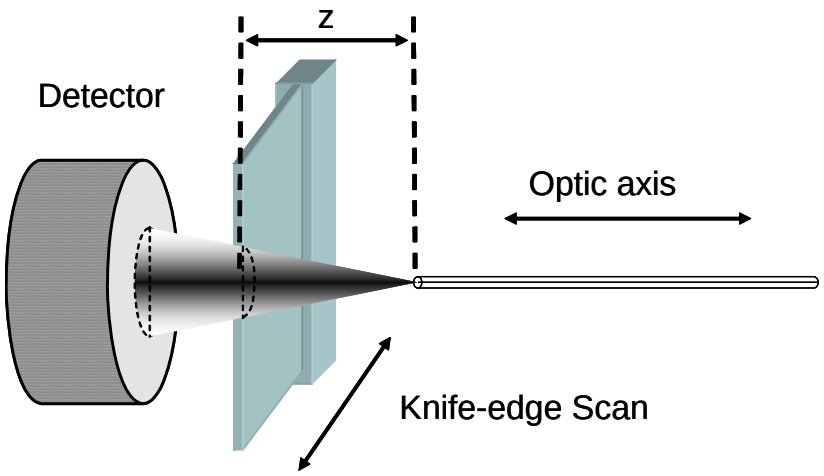

Figure 7. Schematic representation of the knife-edge measurement setup. For regular intervals along the optic axis, the knife-edge was translated into the diverging beam. By monitoring the power on the ~1 cm x 1 cm detector, a measurement of the beam size could be made.

Measurements were taken by initially bringing the fiber to a position that was close to the knife-edge (~ 50 μm as seen under a microscope), and translating the stage back from there, making measurements at regular intervals. At each position, the full amount of optical power on the photodetector was checked to ensure that the beam was fully intersecting the detector. From the total power, the necessary fractional powers to measure the FWHM were calculated. The knife-edge was scanned, using a vernier micrometer with 1 μm resolution, to give the corresponding powers on the detector, and the position of the blade was recorded at those points. The FWHM was then used with Eqn. [9] to determine the 2w beam size. Table 1 shows the raw data, along with the calculated beam diameters.

Distance	12% Position	88% Position	FWHM	Experimental $1/e^2$ Diameter	Theoretical $1/e^2$ Diameter
0	215	225	10	16.98	14.15
50.8	214	230	16	27.17	21.83
101.6	214	233	19	32.27	30.64
152.4	212	237	25	42.46	39.84
203.2	212	241	29	49.26	49.21
254	211	243	32	54.35	58.67
304.8	209	248	39	66.24	68.18
355.6	206	253	47	79.83	77.73
406.4	205	255	50	84.93	87.30
457.2	203	260	57	96.82	96.88
508	201	264	63	107.01	106.48
558.8	200	270	70	118.90	116.08
609.6	197	273	76	129.09	125.69

Table 1. Raw data for the knife edge scan. All values are in μm. The FWHM is found by subtracting the 12% power from the 88% power. Experimental Diameter was found using the FWHM with Eqn. [9]. Theoretical values are for a Gaussian beam with $2w_0$ = 10.5 μm, λ = 1550 nm and a 50 μm offset.

Figure 8 shows the measured beam widths from the knife-edge scan and a comparison to theory for a $2w_0$ = 10.5 μm with a 50 μm offset (approximate distance from fiber end to blade). In this case, both the absolute size of the beam, as well as the slope of the line connecting the data points are in excellent agreement with what is predicted, based on Gaussian beam divergence.

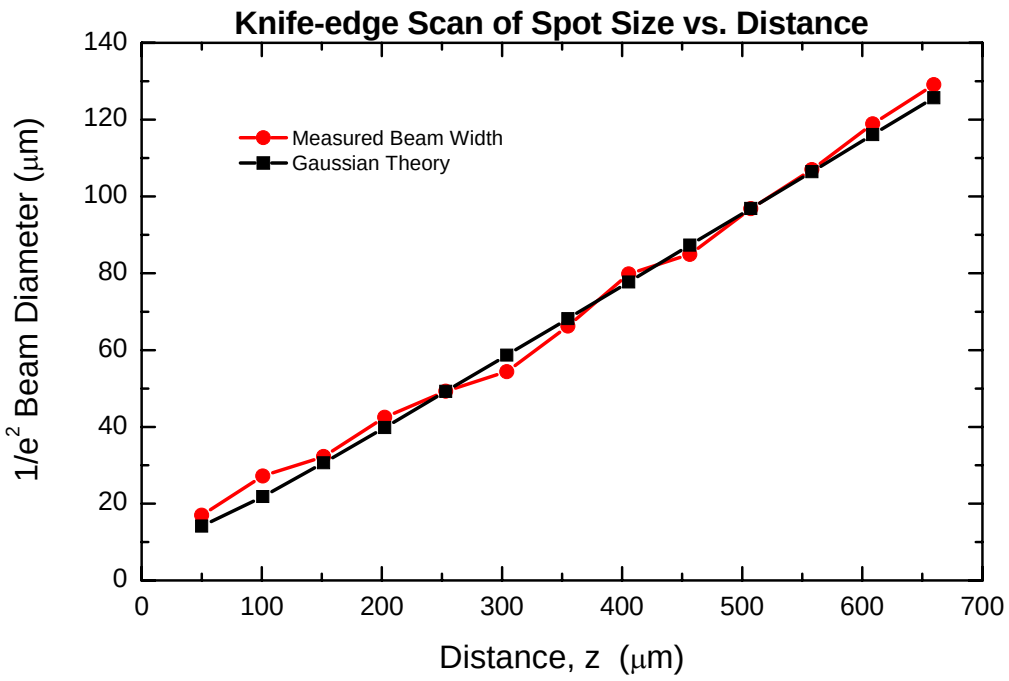

Figure 8. Knife-edge scan beam divergence results (Red Line) compared to theoretical prediction of Gaussian beam divergence (Black Line). Measurements were taken ~50 μm from the blade edge to ~700 μm at regular intervals. The data confirms that there is excellent agreement with theory for a Gaussian beam with $2w_0$ = 10.5 μm.

Pinhole Power Measurement

In the first experiment, a beam profiler was used to characterize the emission from the fiber. Because of its technical complexity, it was impossible to determine if the device was working properly. The results it gave were not only internally inconsistent (between the displayed and saved data), but they were also inconsistent with theoretical predictions. In a more simple second experiment, using only a knife-edge scan, theoretical and experimental data was in excellent agreement. Because of the discrepancy between the results, a third experiment was necessary. To eliminate as many unknowns and to have as simple a setup as possible, a pinhole power measurement was performed.

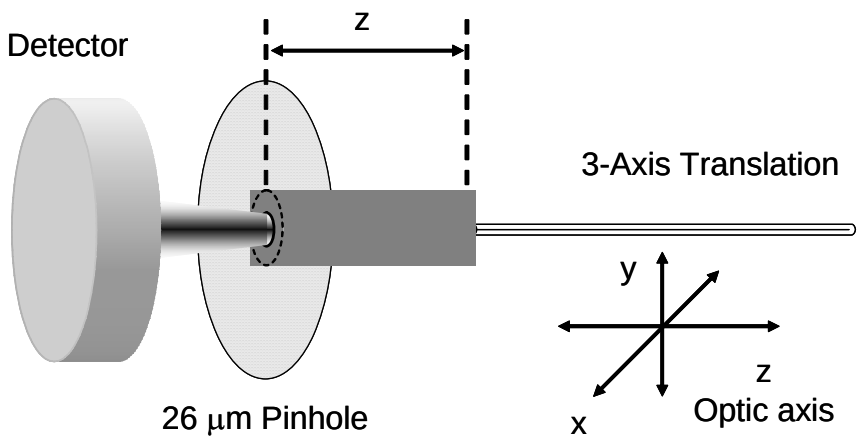

Figure 9. Schematic representation of the pinhole power measurement setup. A pinhole with a measured diameter of 26 μm was placed in front of the output facet of the SMF-28 fiber. By measuring the transmitted power at regular distance intervals from the pinhole, the beam divergence could be determined.

A pinhole, with a measured diameter of 26 ± 1 μm, was placed in front of the fiber output, as shown in Figure 9. A photodetector was placed closely behind the pinhole to collect the transmitted light. The fiber was attached to a 3-axis translation stage and positioned directly next to the pinhole. The distance was increased in regular intervals, and the power transmitted through the hole was maximized by translating along the x and y axes at each position and recorded.

To compare with theory, a Gaussian beam with $2w_0 = 10.5$ μm was analytically propagated over each of the measured distances. At each distance, the power was integrated over an area the size of the pinhole centered on the beam. A similar, but different method was used to compare to the actual fiber mode represented by the Bessel beam. In this case, the Bessel beam defined, by Eqns. [4a and 4b], with the MFD set to 10.5 μm and the total power normalized to unity was used for all calculations. To simulate divergence, the area over which the power was integrated was changed at each distance. The radius of integration at a given distance, z, was estimated by taking the ratio of the pinhole radius to the Gaussian beam radius at that distance, w[z], then multiplying it by the initial $1/e^2$ width of the Bessel beam. For example, at a distance of z = 254 μm, w[z] for a Gaussian beam is 25.8 μm. Dividing this by the pinhole radius of 13 μm and multiplying by the initial mode-field radius of 5.25 μm, gives us a radius of integration of 2.72 μm. By this method, we can effectively scale the Bessel beam with respect to the pinhole size without actually calculating its divergence.

Figure 10 is a plot of the normalized power transmitted through the pinhole vs. distance. All three data sets are in close agreement with each other. The curves that results from the Gaussian beam and the Bessel beam are slightly different because the power in the Gaussian beam is slightly more tightly confined to the central region. This leads to a slightly longer distance of propagation before the detected power drops. The measured data agrees equally well with theoretical plots for the Gaussian and Bessel beams.

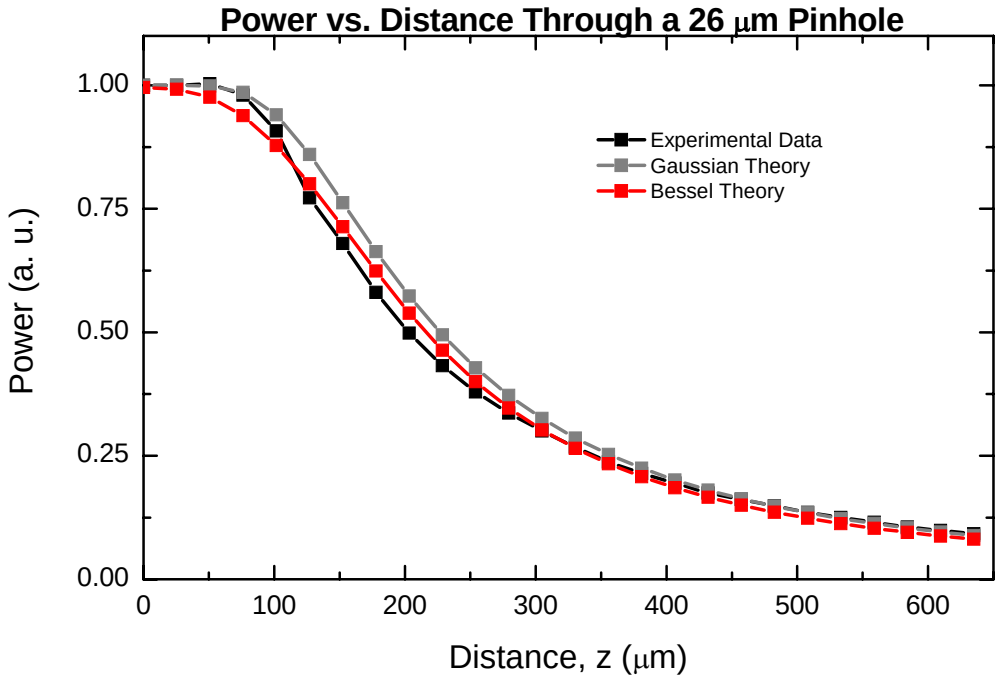

Figure 10. Plot shows predicted power transmitted through a small 26 μm aperture as a function of distance from the pinhole. Both theoretical plots for Gaussian and Bessel beams are shown for the beam parameter $2w_0 = 10.5$ μm. The measured data compares favorably with both theoretical plots

Conclusion

The optical output from an SMF-28 fiber has been characterized using three experiments to determine how well the Gaussian approximation works in predicting beam divergence. The first experiment used a commercial beam measurement system. These results were inconsistent with theoretical predictions. Because the results were also different depending on whether the saved or displayed values were used, it is reasonable to suspect that both measurements are dubious and that the BeamAlyzer should only be used for qualitative and not quantitative analysis.

Because of the failure of the first experiment, a second experiment, which measured the beam size by scanning a single knife-edge, was performed. These results showed excellent agreement with the Gaussian beam approximation. Both spot sizes and the divergence of the beams out to z = 635 μm agreed with the theoretical results based on the specifications of the fiber.

Finally, as an independent check to verify the results of the knife-edge scan, a pinhole power measurement was performed. In this case, the transmitted power through the pinhole was compared with what would be expected for a diverging Gaussian beam, and

also to a Bessel beam. The measured results were in good agreement with both analytical predictions.

Based on the results of the two viable experiments, the Gaussian approximation to the beam that exits an SMF-28 fiber has been shown to be correct to a very high degree. Both $1/e^2$ widths, as well as measured transmitted power through a pinhole verify that the approximation is accurate. Therefore, using a Gaussian beam with a $2w_0$ beam diameter equal to 10.5 mm for SMF28 @ 1.55 μm should be useful for optimizing fiber-to-detector packaging or any other application where knowledge of the characteristics of a beam propagating from the end of a step-index fiber are important.

[1] "Corning SMF-28 Optical Fiber Product Information - PI1036," 2002.

[2] B. Saleh and M. C. Teich, *Fundamentals of Photonics*: John Wiley and Sons, Inc., 1991.

[3] A. Yariv, *Optical Electronics*, 3rd ed. New York: CBS College Publishing, 1985.